

CHAPTER 2

Geocomposite Membrane Effectiveness as a Moisture Barrier

2.1 ABSTRACT

With the advance in electromagnetic techniques, measuring and monitoring the moisture content in pavement systems appears feasible, and geosynthetics contribution to the drainage system can be verified. To investigate the performance of a geocomposite membrane (a low modulus polyvinyl chloride [PVC] layer sandwiched between two nonwoven geotextiles), two sections at the Virginia Smart Road were instrumented and were constructed to quantify its effectiveness as a moisture barrier and as a strain energy absorber. All layers were instrumented for stress and strain measurements as well as for environmental effects (temperature, frost, and moisture). The moisture variation in the subbase aggregate layer over different precipitations was continuously monitored using time domain reflectometry. Ground penetrating radar (GPR) was also periodically used to monitor water movement in the pavement sections. Results of the GPR surveys indicated that using a geocomposite membrane underneath a drainage layer forms a water barrier, thus preventing the saturation of underlying layers and facilitating the lateral drain of water. Furthermore, the results of time domain reflectometer moisture sensors validated the effectiveness of the geocomposite membrane in abating water infiltration into the subbase layer even in the event of heavy rain. Long-term effectiveness of the geocomposite membrane was also investigated and discussed over a monitoring period of 20 months.

2.2 INTRODUCTION

Excessive moisture in a pavement structure and inadequate drainage systems have been identified as major sources of failure in flexible pavements (Marienfeld and Baker 1999). Moisture damages a pavement structure by weakening the subgrade soil and aggregate layers, resulting in lower shear strength of the material and insufficient subgrade bearing capacity to sustain loading and unloading cycles. In addition, undrained layers result in less distribution of load. Although moisture is the main cause of many pavement distresses (e.g. stripping in hot-mix asphalt [HMA] layers, loss of subgrade support, reduction of load-carrying capacity during frost melting period, etc.), it is practically difficult to quantitatively include in pavement design and rehabilitation methods. This difficulty has led to generally ignoring the moisture problem during pavement rehabilitation, which may result in the appearance of the original problem after an unsatisfactory service life. To address this high cost of repair, it has been recognized that drainage is an issue to be mainly addressed by adequate original design and construction practices (Marienfeld and Baker 1999).

Nowadays, drainage systems, such as permeable aggregate bases (asphalt or Portland cement treated) and edge drains, are becoming a common addition to flexible pavement design. In addition to these drainage practices, the use of geosynthetic materials may be beneficial. Geosynthetics are thought to provide five distinct functions in pavement and bridge systems: reinforcement of a particular layer, separation (by maintaining the integrity of particular layers by preventing intermixing), drainage or filtration, stress absorption, and a moisture barrier. There are currently three types of geosynthetic materials, which have been designed to perform drainage functions: geotextiles (woven or nonwoven), geonets, and geocomposites, which combine the main function of different geosynthetics to obtain a multi-purpose fabric.

Although moisture in pavements is one of the most important factors in pavement performance, it is extremely difficult to monitor or to measure after pavement construction. With the advance in electromagnetic techniques, moisture monitoring using time-domain reflectometry (TDR) and ground-penetrating radar (GPR) appears more

feasible. In 1999, Al-Qadi and Loulizi employed a ground coupled impulse system with a 900-MHz center frequency to detect the presence of moisture within pavement systems (Al-Qadi and Loulizi 1999). The GPR system successfully detected pavement sub-drainage related distresses. In 1996, Hagen and Cochran effectively used time domain reflectometry probes to study the performance of different drainage systems (Hagen and Cochran 1996).

Although some of the geosynthetic benefits can be easily identified by observing the overall performance of a pavement, the drainage capability of geosynthetics has long been a source of debate as it is virtually impossible to verify. While some studies indicated the waterproofing benefits provided by geosynthetics based on laboratory and field investigations (Forsyth et al. 1987; Phillips 1993), other studies have suggested that the evidence that impermeable fabric interlayers result in less moisture content in road bases was yet to be seen (Kennepohl et al. 1985). This part of the dissertation illustrates and validates the effectiveness of a specially designed geocomposite membrane system as a moisture barrier in flexible pavement systems. The geocomposite membrane was installed in 1999 for the first time in the U.S. at the Virginia Smart Road test facility.

2.3 BACKGROUND

The Virginia Smart Road, located in Southwest Virginia, is a unique state-of-the-art full-scale research facility for pavement research and evaluation of Intelligent Transportation Systems (ITS) concepts, technologies, and products. It is the first facility of its kind to be built from the ground up with its infrastructure incorporated into the roadway. When completed, the Virginia Smart Road will be a 9.6-km connector highway between Blacksburg and I-81 in Southwest Virginia, with the first 3.2km designated as a controlled test facility. The flexible pavement part of the Virginia Smart Road test facility includes 12 heavily instrumented flexible pavement sections; see Table 2-1. Section length varies between 76 and 117m, with the exception of section A, which is 317m. Seven of the 12 sections are located on a fill, while the remaining five sections are located in a cut. Different layers are used in each section (all designations and mix

designs are in accordance with Virginia Department of Transportation Specifications). The different layers are as follows:

- Wearing surface: Seven types of HMA wearing surface are used (SM-9.5A, SM-9.5A with high laboratory compaction, SM-9.5D, SM-9.5E, SM-12.5D, SMA-12.5, and open-graded friction course [OGFC]). Five of these seven mixes are SuperPave™ mixes. All of the mixes, with the exception of the OGFC, were constructed at 38-mm-thick. The OGFC was constructed at 19-mm-thick.
- Intermediate HMA layer: BM-25.0 at different thickness ranging from 100 to 244 mm.
- Three sections have the SuperPave™ SM9.5A fine mix placed under the BM-25.0 to examine the benefits of such a design on reducing fatigue cracking.
- Open-graded drainage layer [OGDL]: Out of the 12 sections, three sections were built without OGDL. Seven sections are treated with asphalt cement and two are treated with Portland cement. The thickness of this layer is kept constant at 75mm throughout the project.
- Cement Stabilized Subbase: 21-A cement-stabilized layer is used in 10 sections at a thickness of 150mm.
- Subbase layer: 21-B aggregate layer was placed over the subgrade at different thickness with and without a geosynthetic.

As the construction of the first phase of this project is completed (3.2km controlled test facility), the Virginia Smart Road is currently used as a test facility by allowing only controlled traffic loading to pass over the different pavement sections. Among the 12 heavily instrumented sections, four sections were built with different interlayer products (see Table 2-1). More than 500 instruments were embedded in the road during construction to quantitatively measure the response of the pavement sections to vehicular loading under different environmental conditions.

Table 2-1. Pavement Design at the Virginia Smart Road

Section	Station Starts	Station Ends	Bunker Station	Lane Length (m)	Surface 38mm	BASE BM-25.0 (mm)	BASE SM-9.5A (mm)	OGDL (mm)	21A Aggr. Cem. Stab. (mm)	21-B Aggr. (mm)	Pave. Thick. (mm)	Fill/ Cut
A	100.54	103.71	103.71	104	SM-12.5D	150	0	75	150	175	588	Fill
B	103.71	104.61	103.71	90	SM-9.5D	150	0	75	150	175/GT	588	Fill
C	104.61	105.48	105.48	87	SM-9.5E	150	0	75	150	175/GT	588	Fill
D	105.48	106.65	105.48	117	SM-9.5A	150	0	75	150	175/GT	588	Fill
Bridge	106.65	107.70										
E	107.70	108.46	108.46	76	SM-9.5D	225	0	0	150	75/GT	488	Fill
F	108.46	109.40	108.46	94	SM-9.5D	150	0	0	150	150	488	Fill
G	109.40	110.30	110.30	90	SM-9.5D	100	50	0	150	150/GT	488	Fill
H	110.30	111.20	110.30	90	SM-9.5D	100	50	75	150	75	488	Cut
I	111.20	112.18	112.18	98	SM-9.5A*	100/RM	50	75	150	75	488	Cut
J	112.18	113.10	112.18	92	SM-9.5D	225	0	75	0/MB	150	488	Cut
K	113.10	113.96	113.96	86	OGFC+SM-9.5D	225/SR	0	75 (Cement)	0	150	488	Cut
L	113.96	115.00	113.96	104	SMA-12.5	150/RM	0	75 (Cement)	150	75	488	Cut

* High lab compaction

SR: Stress Relief Geosynthetic; GT: Woven Geotextile/ Separator; RM: Reinforcement Mesh; MB: Moisture Barrier

CRCP: Continuously Reinforced Concrete Pavement

For successful instrumentation strategy, at least two types of response (stress, strain or deflection) should be compared simultaneously. Therefore, strain and stress were carefully monitored along the depth of the pavement system. Also, climatic parameters, including temperature, moisture, and frost depth were monitored at different depths along the pavement. Two different types of TDR probes were used at the Virginia Smart Road: CS615 and CS610 probes. One may refer to Al-Qadi et al. (2001) and Loulizi et al. (2001) for further details about the Virginia Smart Road construction and instrumentation. In addition, detailed description of the instrumentation and calibration at the Virginia Smart Road is presented in Appendix A.

The Virginia Smart Road offers an opportunity to explore the effectiveness of a specially designed geocomposite membrane as a moisture barrier. This membrane consists of a 2-mm-thick low modulus polyvinyl chloride (PVC) backed on both sides with 150g/m² polyester nonwoven geotextile. The primary function of the PVC geocomposite membrane is to control water infiltration or fine migration. Typical values of geocomposite membrane permeability were reported between 1×10^{-13} and 2×10^{-13} cm/sec. The geocomposite membrane was installed in two different sections at the Virginia Smart Road. In section J, a geocomposite membrane was installed underneath an asphalt treated drainage layer to test its effectiveness as a moisture barrier. In section K, the geocomposite membrane was installed within the HMA base to investigate its capability to relieve stresses (see Chapter 3); a schematic of the layered system of section J is presented in Figure 2-1 (all designations are in accordance with Virginia Department of Transportation specifications). This geocomposite membrane has been successfully used as impermeable material for dams, canals, reservoirs, and hydraulic tunnels (Scuero and Vaschetti 1997). While this geocomposite membrane has been used on two bridge decks in Italy, it has never been used on any roads or bridges in the United States, prior to its installation at the Virginia Smart Road pavement test facility.

2.4 GEOCOMPOSITE INSTALLATION

Prior to the installation of the geocomposite membrane, a 75-mm of 21-B granular subbase was installed in section J. This is a common environment for the placement of a moisture barrier. At this location, the interlayer should protect the granular layers (subbase and subgrade) from the intrusion of rainwater coming from the top layers. It should be noticed, however, that the use of a moisture barrier is not justified if a high water table is detected since in this case, the water may infiltrate from the bottom layers to the granular materials.

The following installation procedure used at the Virginia Smart Road was newly developed due to the lack of familiarity with the installation of such materials in roadways. The layout of the installation in the two sections was similar: five rolls, 37m-long and 2.05m-wide each, were installed over the complete width of the road and 2.15m into the shoulder; and additional rolls were installed to achieve a 50-meter long installation.

It rained on and off during the day of the geocomposite membrane installation (August 25, 1999). However, rainy conditions did not affect deployment of the rolls. The temperature was approximately 25°C. Prior to installation, the area to be covered with geocomposite membrane was carefully cleaned of any loose aggregates. The installation of the geocomposite membrane in section J (moisture barrier over a granular material) did not necessitate the use of a prime coat between the geotextile and the underneath layer (21-B aggregate subbase layer). A prime coat may not be effective when applied to a granular material (e.g., 21-B) because greater friction may exist between the geocomposite membrane and the aggregate layer when the prime coat is absent.

The deployment of the rolls was easy and accurate because the rolls could be moved slightly after being laid. Installation of the roll over the instruments was critical to avoid any damage to the instruments. It was decided to install the roll one meter away from the exact lateral location to avoid any damage to the instruments by the installing vehicle. The roll was then pulled back to its exact location. Transverse joints between

PVC rolls were staggered to prevent the creation of a weak joint across the pavement lane. An overlap of 85mm was made at the transverse joints. At the longitudinal joints, a 55mm length welding was performed by applying hot air to melt the uncovered PVC end. The welding of the material for a 10-m-wide by 50-m-long section took five to six hours and was carefully checked using screwdrivers.

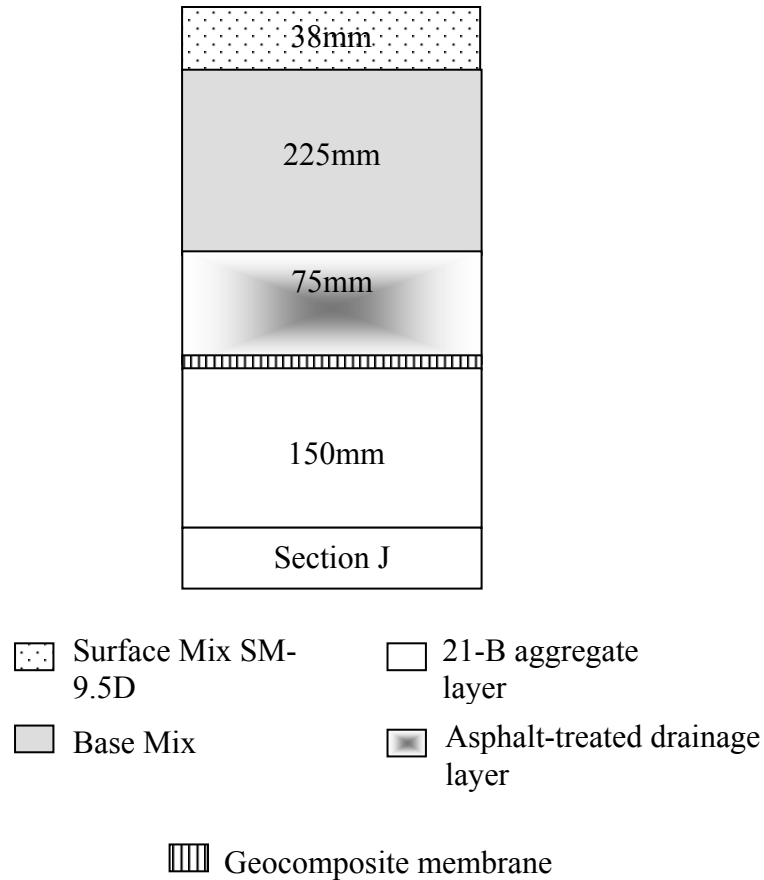


Figure 2-1. Pavement Design for Section J

Sandbags were placed over the geocomposite membrane to keep it in place prior to the surface prime coat application. Sandbags held the geocomposite membrane in place and the sand was used later to prevent the membrane from being picked up by truck tires during paving. It rained during this time, but the geocomposite material was covered with plastic sheets until prime coating. Temperature and moisture sensors were placed on

both sides of the geocomposite membrane, while three pressure cells (500mm apart in the traffic direction and 300mm apart in the wander area) were installed under the geocomposite membrane. Instruments were installed prior to the placement of the geocomposite membrane, after which cuts were made to allow the instruments to be placed on top of the membrane. The cuts were then welded using adhesive geosynthetics and tack coat. The upper surface of the geocomposite membrane was primed using PG 64-22 asphalt binder at an application rate of 1.5 kg/m² after one week (see Figure 2-2).



Figure 2-2. Prime Coat Application on Top of the Geocomposite Membrane in Section J

Seventy-five millimeters of asphalt-treated drainage layer were then placed on top of the geocomposite membrane (see Figure 2-3). It was obvious on the day of paving that the geocomposite membrane was being picked up by the trucks delivering HMA to the paving machine. Sand was placed over the geocomposite membrane where the truck wheel paths were. This prevented the tires from adhering to the geocomposite membrane and lifting it. Such a practice may be needed when no prime coat is used underneath the geocomposite membrane. The lifting of the geocomposite membrane would have been worse if the rolls were not welded together to create one large, heavy sheet of material.

After the placement of the asphalt-treated drainage layer, three lifts of 75mm of BM-25.0 were installed, followed by a 38mm surface mix (SM-9.5D). No problems occurred during the installation of the instruments and no sensors were lost during construction in this section. In general, the installation of the instruments was very successful with a total loss of less than 5% during construction and less than 14% after one year of service. This number is very low when a loss of 50% is not unusual (Ullidtz 1987).



Figure 2-3. Installation of the Open-Graded Drainage Layer in Section J

In this chapter, the effectiveness of the geocomposite membrane as a moisture barrier is evaluated by two methods: ground penetrating radar (GPR) and time domain reflectometer (TDR).

2.5 MOISTURE DETECTION BY GROUND PENETRATING RADAR

Ground penetrating radar was periodically used to monitor water movement in the pavement sections at the Virginia Smart Road and to identify any significant changes in the pavement system profile. Two GPR types (900 MHz ground-coupled and 1 GHz air-

coupled) were used in this project; see Figure 2-4. This technique is based on sending electromagnetic waves through the surveyed structure and then analyzing the reflected signal (Loulizi et al. 1999). The velocity of electromagnetic waves in a material can be estimated as follows:

$$v = \frac{c}{\sqrt{\epsilon_r}} \quad (2.1)$$

where

v = speed of propagation of the wave (m/s);

c = speed of an electromagnetic wave in free space (3×10^8 m/s); and

ϵ_r = relative permittivity (dielectric constant) of the traveling medium.

When an electromagnetic wave travels through two different materials, energy will be reflected and transmitted at the interface. The degree of reflection depends on the dielectric constants of the two materials. This is approximated as follows:

$$r = \frac{\sqrt{\epsilon_{r1}} - \sqrt{\epsilon_{r2}}}{\sqrt{\epsilon_{r1}} + \sqrt{\epsilon_{r2}}} \quad (2.2)$$

where

r = degree of reflection;

ϵ_{r1} = relative permittivity of the first layer; and

ϵ_{r2} = the relative permittivity of the second layer.

Equations (2.1) and (2.2) are considered the basis for interpreting GPR data. From Equation (2.1), one can calculate either the unknown thickness of a given layer (knowing the dielectric constant) or the dielectric constant of a given layer (knowing the exact thickness). On the other hand, Equation (2.2) is used to determine if moisture

accumulation exists in a given layer by monitoring the changes in the amplitude of the reflected signal. Free water has a very high dielectric constant (81) compared to construction materials (3-8).



Air Coupled System (1GHz)



Ground Coupled System (900MHz)

Figure 2-4. Ground Penetrating Radar Systems Used at the Virginia Smart Road

2.6 MOISTURE BARRIER EVALUATION USING GPR

Based on this aforementioned simplified approach and a more detailed one (Al-Qadi et al. 2000), two sections with and without geocomposite membrane system were compared. Figure 2-5 illustrates a scan taken at the pavement surface after a rainy day in section J (with geocomposite membrane). In this scan, the uniformity of the color refers to the absence of any abnormal spots (i.e. water accumulation and voids, etc.). It is clear from this figure that water did not accumulate in the overlying layers (e.g. OGDL) prior to drain laterally. It is thought that accumulation of the water in the overlying layers may only occur if the layer lateral slopes are not adequately designed. The lateral slope is 2% at the Virginia Smart Road.

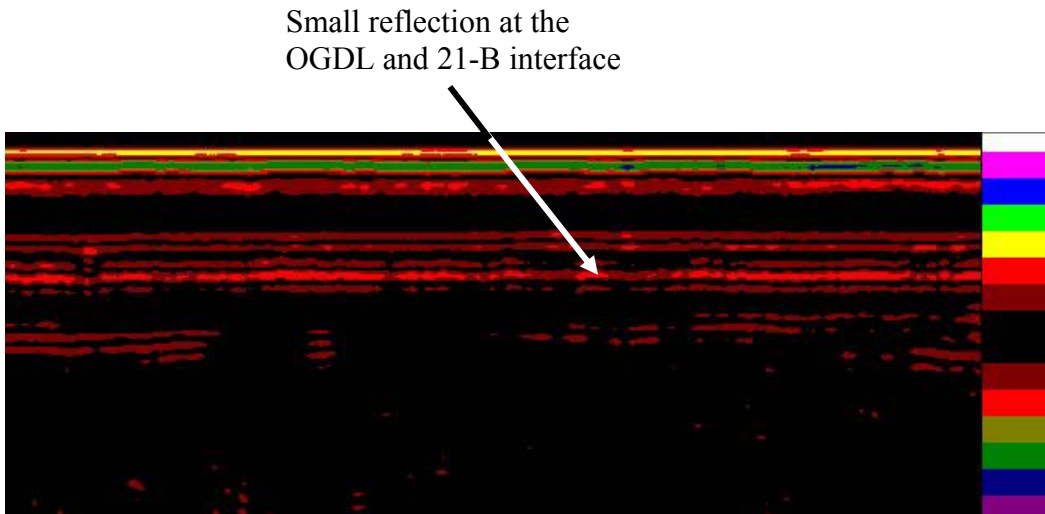


Figure 2-5. GPR Survey on Top of the Geocomposite Membrane in Section J

Conversely, Figure 2-6 presents a scan taken for a similar pavement section but without the geocomposite membrane (section B). As one may note in this case, a high reflection (shown by an arrow) due to moisture presence appears at the interface between the drainage layer (OGDL) and the underneath layer (21-B aggregate layer). This indicates that the 21-B layer has high moisture content, which may not be desirable as it will reduce the resilient modulus of that layer and, hence, the structural capacity of the pavement system. In addition, the presence of moisture in this layer may result in clogging part of the drainage layer due to fine particles movement and pumping. It appears that an effective water barrier may solve such problems by preventing the saturation of underlying layers and forcing the water to drain laterally to a shoulder drain system given that the water table level is low.

The capability of the geocomposite membrane to act as a moisture barrier was also detected in section K. As previously clarified, the geocomposite membrane was installed in this section to examine its ability to reduce the transverse tensile strain in the HMA layer due to its strain energy absorption capability, which is presented in Chapter 3. Figure 2-7 shows that the geocomposite membrane acts as a moisture barrier in this section preventing the infiltration of water to the underlying layers. The role of the drainage layer seems to be significantly reduced since water is already removed from the pavement system at shallow depth through the geocomposite membrane and the

OGFC layer. However, one needs to be careful not to develop stripping in the HMA layer because of entrapped water.

High moisture content at
OGDL and 21-B interface

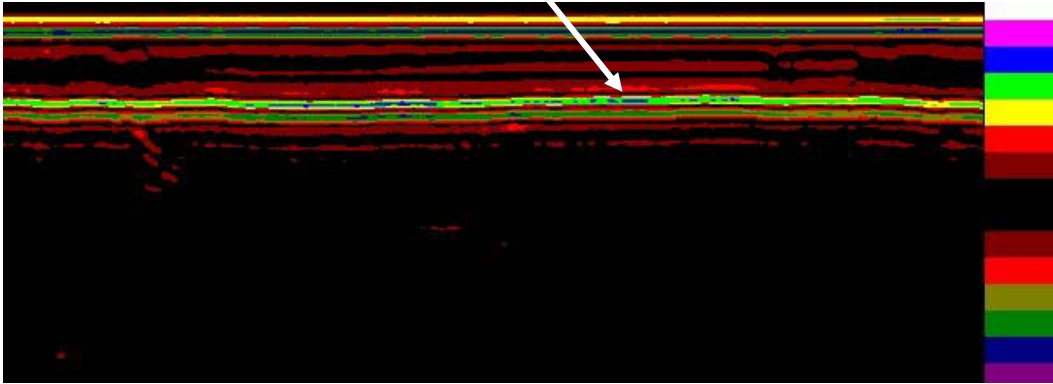


Figure 2-6. GPR Survey on a Section without Geocomposite

Small reflection at OGDL-
21-B interface

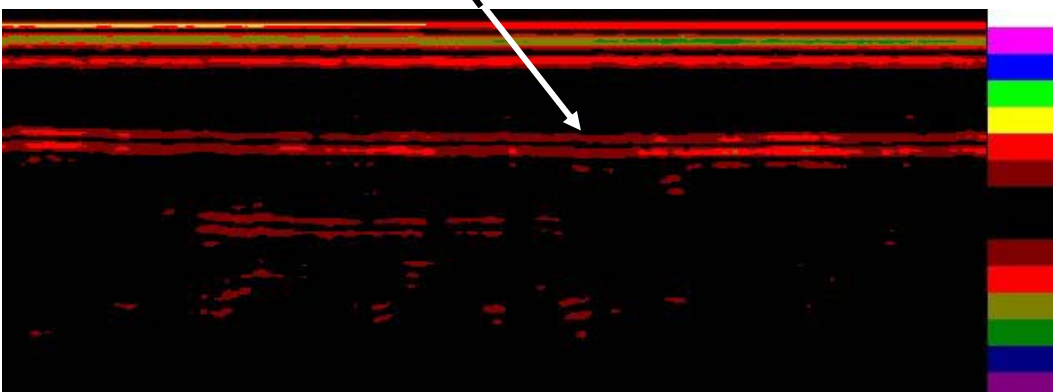


Figure 2-7. GPR Survey on Top of the Geocomposite Membrane in Section K

2.7 MOISTURE DETECTION BY TIME DOMAIN REFLECTOMETER

Subbase and subgrade moisture contents were measured using time domain reflectometers (TDRs). Time domain reflectometer probes consist of two or more stainless steel rods that are inserted in the host material. The soil moisture content is evaluated by sending a pulsed signal in the host material and examining the reflection of the signal. Since the amplitude and frequency of the reflected signal are based on the dielectric properties of the host material, the measurements can be related to soil moisture content. The dielectric constant of dry aggregates ranges from 4 to 8 depending on the mineral compositions, and the dielectric constant of wet aggregates can reach up to 20. This conversion may rely on equations provided by the manufacturer (with an accuracy of $\pm 2\%$). However, greater accuracy can be achieved by developing calibration equations from comparisons between moisture contents using TDR method and gravimetric methods (oven drying).

Two types of TDR probes were used at the Virginia Smart Road: the traditional CS610 and the newly developed CS615 (see Figure 2-8). The CS610 water content reflectometer consists of three conducting rods that are 300mm in length. Output from the CS610 TDR is usually displayed as a voltage or reflection coefficient versus time. To obtain the volumetric moisture content from the probe output, use can be made of the universal equation proposed by Topp et al. (1980):

$$\theta_v = -5.3 \times 10^{-2} + 2.92 \times 10^{-2} \varepsilon_a - 5.5 \times 10^{-4} \varepsilon_a^2 + 4.3 \times 10^{-6} \varepsilon_a^3 \quad (2.3)$$

where

θ_v = volumetric moisture content (percent); and

ε_a = apparent dielectric constant that is defined as follows (Topp et al. 1980):

$$\varepsilon_a = \left(\frac{ct}{2l} \right)^2 \quad (2.4)$$

where

c = velocity of an electromagnetic wave in free space (3×10^8 m/s);

l = length of the TDR transmission line (m); and

t = two-way travel time of the electromagnetic wave as measured by the TDR system (sec).



(a)

(b)

Figure 2-8. Configuration of the TDR Probes Used at the Virginia Smart Road: (a) CS610 and (b) CS615

The CS615 consists of two parallel conducting rods that are also 300mm in length. Output from the CS615 is usually displayed as frequency. The output from the probes can be converted into the volumetric moisture content by using the equations provided by the manufacturer (with an accuracy of $\pm 2\%$). Greater accuracy can be achieved by developing calibration equations from comparisons between moisture contents using the TDR method and gravimetric methods. Such calibration equations were developed for the 21-B granular materials used at the Virginia Smart Road (Diefenderfer et al. 2000). The CS615 probes were calibrated for a volumetric moisture content ranging from 1% to 20%. Different calibration equations (second and third order) were developed from the laboratory-obtained data (Diefenderfer et al. 2000):

$$\theta_v = -0.6816t^2 + 1.7907t - 0.9692 \quad (2.5)$$

$$\theta_v = 5.6821t^3 - 17.267t^2 + 17.767t - 6.0495 \quad (2.6)$$

where

t = time in msec; and

θ_v = volumetric moisture content.

The obtained coefficients of determination (R^2) for the developed equations ranged between 0.97 and 0.99. Although the results from the two probes are correlated, this study only presents the results from the CS615 probe, as it provides continuous data and can be easily connected to a data acquisition system.

2.8 MOISTURE BARRIER EVALUATION USING TDRs

The developed calibration models were used in predicting the volumetric moisture content based on the periodic measurements taken from the field. Although the OGDG layers are also instrumented for moisture measurements, the focus in this chapter is on the water infiltration to the aggregate layer. Two sections with and without geocomposite membrane were compared. Moisture data are continuously collected from the data acquisition system every 60minutes. Figure 2-9 shows the collected data for two CS615 probes in the 21-B aggregate layer of section B along with the precipitation occurring over the same period of time. As noticed from this figure, the measured moisture content in the 21-B aggregate layer is highly dependent on the amount of precipitation received. For instance, a large increase in moisture content (around 5%) occurred on this section after a rain event on April 17, 2000. This large moisture content may significantly reduce the bearing capacity of the subbase and the subgrade, causing progressive failure of the pavement. Cedergren (1974) predicted a reduction of 50% in the pavement service life if a pavement base is saturated as little as 10% of the time.

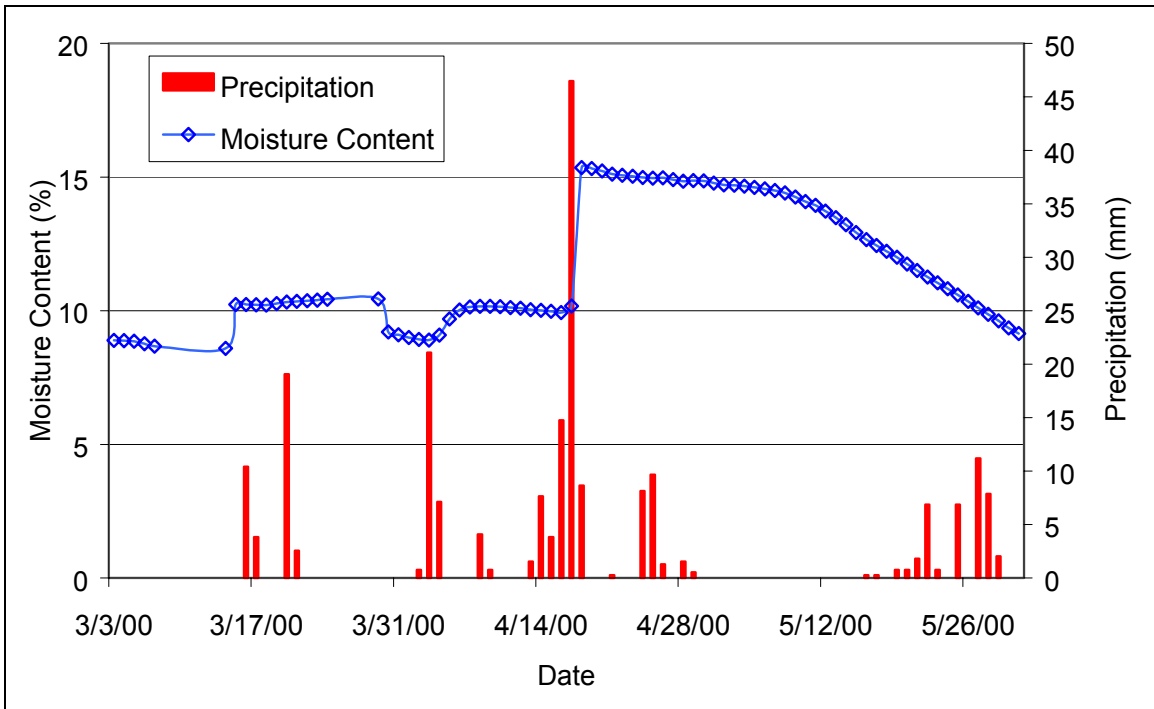


Figure 2-9. Moisture Measurements in Section B along with the Precipitation Occurring over the Same Period of Time (from March 3rd 2000 to May 31st 2000)

Conversely, Figure 2-10 illustrates the moisture content data for the CS615 probes in the 21-B layer of section J (similar in design to section B but with geocomposite membrane) along with the precipitation occurring over the same period of time. As noticed from this figure, the moisture content remained nearly constant over the entire monitored period. Even after the high rain event of April 17, 2000, the measured moisture content in the 21-B aggregate layer remained at the same level. This figure indicates the effectiveness of the geocomposite membrane in maintaining constant moisture content (below the optimum) over different precipitation periods. The same trend was also observed in section K (Figure 2-11). The measured moisture content was independent from the amount of rainwater, which is the primary source of moisture in pavement structures that have a low water table.

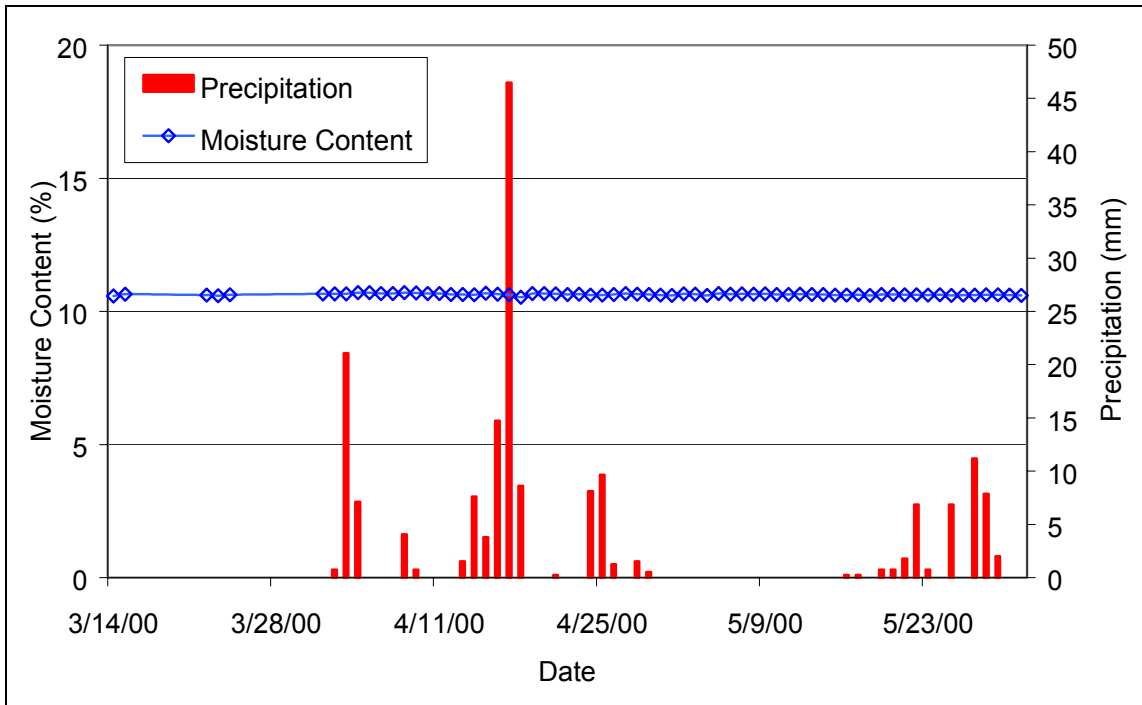


Figure 2-10. Moisture Measurements in Section J along with the Precipitation Occurring over the Same Period of Time (from March 3rd 2000 to May 31st 2000)

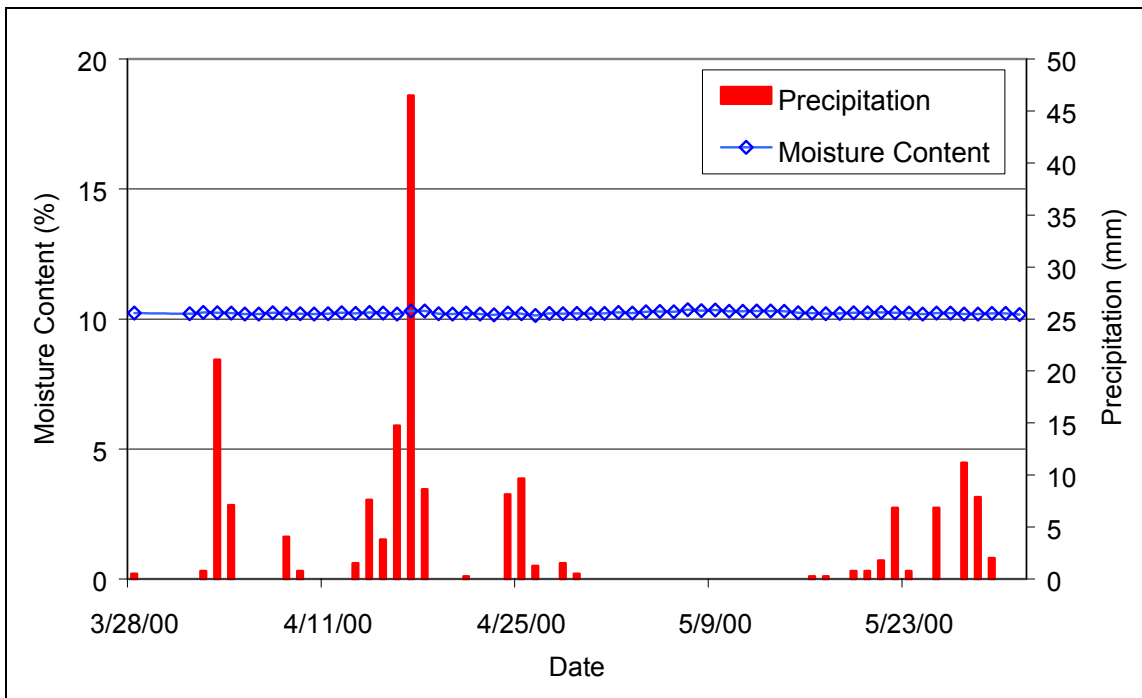


Figure 2-11. Moisture Measurements in Section K along with the Precipitation Occurring over the Same Period of Time (from March 3rd 2000 to May 31st 2000)

2.9 LONG TERM MONITORING

The long-term effectiveness of the geocomposite membrane to function as a moisture barrier was investigated and monitored from January 2000 to August 2001. Different months of interest, in which the amount of precipitation was significant, were analyzed. Figures 2-12 to 2-14 illustrate the measured moisture content along with the precipitation occurring over different periods of time. Based on the long-term monitoring period, the following observations may be made:

1. The measured moisture content in section J (section with geocomposite membrane) was relatively constant (from 8 to 10%) over the entire monitoring time period. This indicates the effectiveness of the geocomposite membrane in maintaining constant volumetric moisture content (below the optimum) over different precipitation periods.

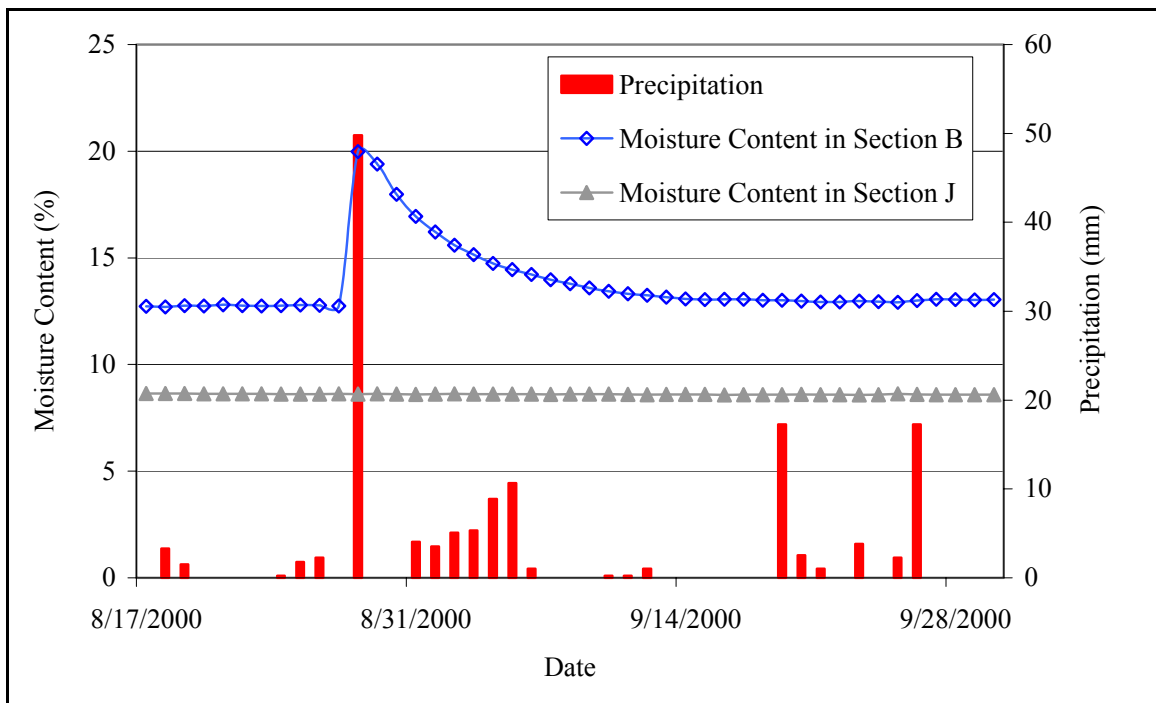


Figure 2-12. Moisture Measurements in Section B and J along with the Precipitation Occurring over the Same Period of Time (from August 17th 2000 to September 30th 2000)

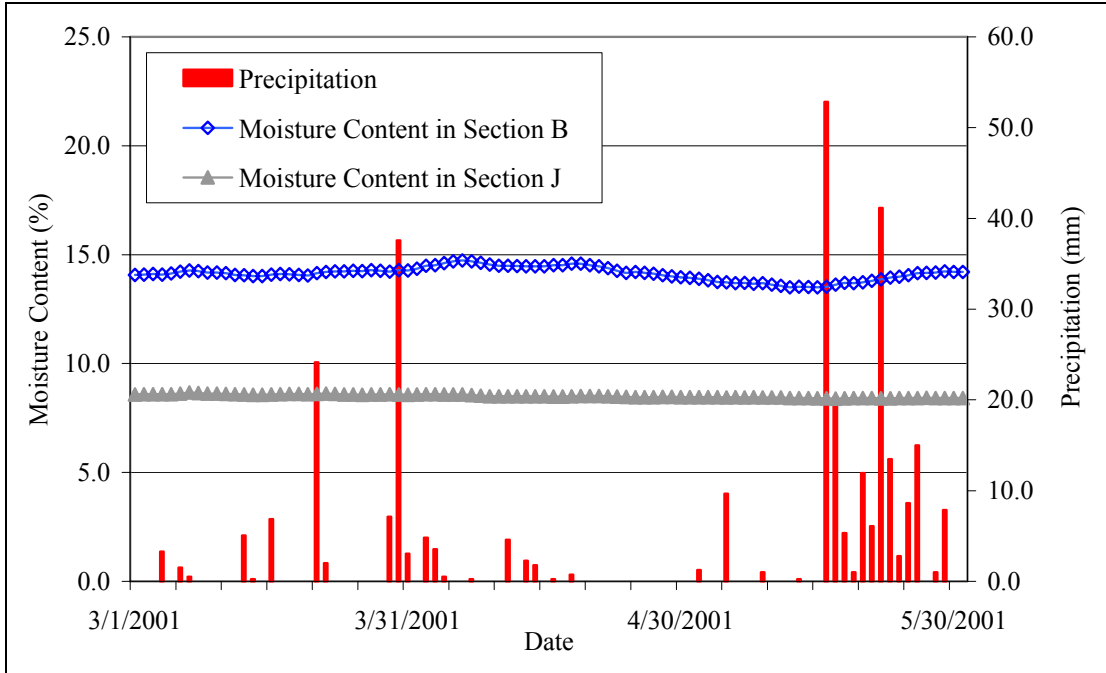


Figure 2-13. Moisture Measurements in section B and J along with the precipitation occurring over the same period of time (from March 1st 2001 to May 31st 2001)

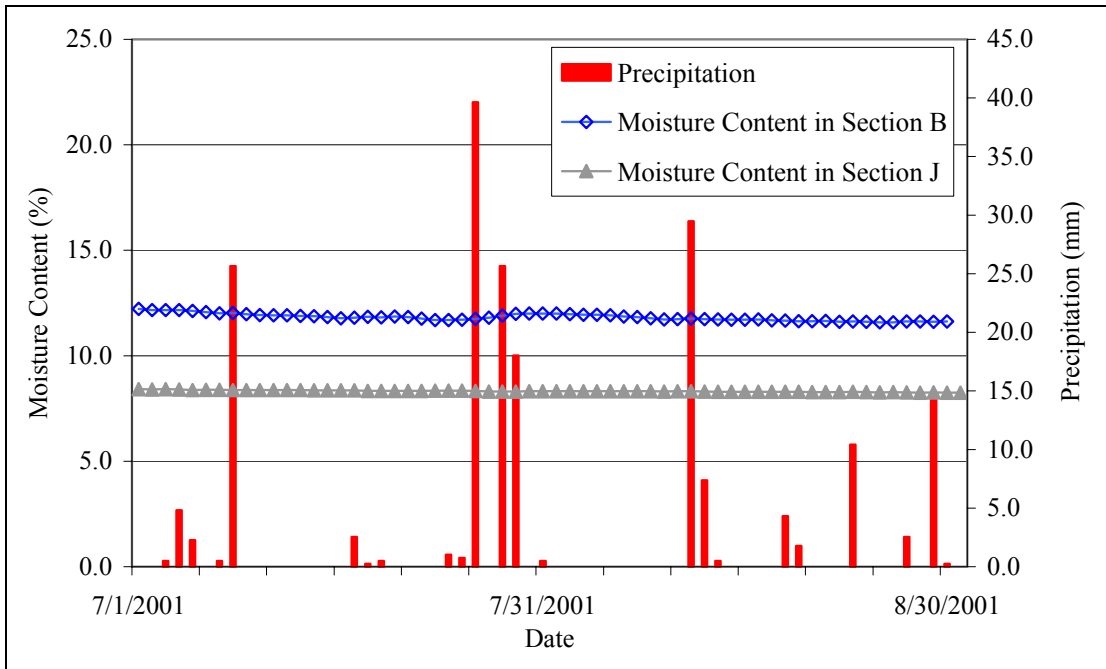


Figure 2-14. Moisture Measurements in Section B and J along with the Precipitation Occurring over the Same Period of Time (from July 1st to August 31st 2001)

2. The measured moisture content in section B (section without geocomposite membrane) appeared to stabilize with time: although the measured moisture content was highly dependent on the amount of precipitation received during the first year (see Figures 2-9 and 2-12), it appeared that the amount of moisture in the granular layer started to stabilize (see Figures 2-13 and 2-14). This may be due to a partially clogging problem within the drainage layer, which prevented the water to infiltrate to the granular layer and mainly because the measured moisture in the granular layer was close to saturation.

2.10 FINDINGS AND CONCLUSIONS

The following findings are based on the field installation and evaluation of the geocomposite membrane:

- Ground-penetrating radar surveys indicate the effectiveness of the specially designed geocomposite membrane to prevent water infiltration to the underlying layers and successfully drain the water to the shoulder.
- Time domain reflectometry confirmed the ability of the geocomposite membrane to effectively protect underneath layers from water accumulation and moisture damage.
- A pavement drainage system composed of a permeable asphalt-treated drainage layer backed by a geocomposite membrane appears capable of removing drainable water from the pavement system, and provides a dry service condition for the underneath layers even in the event of heavy rain.
- Over the entire 20-month monitoring period, the measured volumetric moisture content was relatively constant (from 8 to 10%) when the geocomposite membrane was used. This confirms the long-term effectiveness of the geocomposite membrane to act as a moisture barrier.

This study concludes that a water barrier is essential underneath an open-graded drainage layer (OGDL) to prevent water infiltration to the subbase and subgrade materials. The use of a drainage layer without any precautions for water filtration appears risky; the use of a moisture barrier for such purposes has proven effective and needed. However, a thinner product that has a 4.5 to 5m width is recommended to facilitate the installation procedure. Installation of the geocomposite membrane has been previously researched using a discrete event simulation procedure, and has been presented elsewhere (Wanamakok et al. 2001).

The geocomposite membrane proved to be able to prevent water infiltration even if installed in the upper HMA layer; however, the water should be drainable, otherwise it may cause stripping in the HMA. This capability offers the potential to use this type of geocomposite membrane as a multi-purpose system: water barrier and strain energy absorption. The latter has yet to be evaluated and presented in Chapter 3.

2.11 REFERENCES

- Al-Qadi, I. L., and Loulizi, A. (1999). "Using GPR to evaluate the effectiveness of moisture barriers in pavements." *Structural Faults and Repair 99*, 8th International Conference, Forde, M. C., editor, London, England, July 13-15.
- Al-Qadi, I. L., Flintsch, G. W., Loulizi, A., Lahouar, S., and Nassar, W. (2001). "Pavement instrumentation at the Virginia Smart Road." *14th IRF Road World Congress*, Paris, France.
- Cedergren, H. R. (1974). *Drainage of highway and airfield pavements*, John Wiley & Sons, New York, NY.
- Diefenderfer, B. K., Al-Qadi, I. L., and Loulizi, A. (2000). "Laboratory calibration and field verification of soil moisture content using time-domain reflectometry." *Transportation Research Record 1699*, Transportation Research Board, Washington, D.C., 142-150.
- Forsyth, R. A., G. K. Wells, and Woodstrom, J. H. (1987). "Economic impact of pavement subsurface drainage." *Transportation Research Record 1121*, Transportation Research Board, Washington, D.C., 77-85.
- Hagen, M. G., and Cochran, G. R. (1996). "Comparison of pavement drainage systems." *Transportation Research Record 1519*, Transportation Research Board, D.C., 1-10.
- Kennepohl, G., Kamel, N., Walls, J., and Hass, R. C. (1985). "Geogrid reinforcement of flexible pavements design basis and field trials." *Proc., Annual Meeting of the Association of Asphalt Paving Technologists*, Vol. 54, San Antonio, TX, 45-75.

- Loulizi, A., Al-Qadi, I. L., Bhutta, S. A., and Flintsch, G. W. (1999). "Evaluation of geosynthetics used as separators." *Transportation Research Record 1687*, Transportation Research Board, Washington, D.C., 104-111.
- Loulizi, A., Al-Qadi, I. L., Lahouar, S., Flinstch, G. W., and Freeman, T. E. (2001). "Data collection and management of the instrumented Smart Road flexible pavement sections." *Journal of the Transportation Research Record 1769*, Transportation Research Board, Washington, D.C., 142-151.
- Marienfeld, M. L., and Baker, T. L. (1999). "Paving fabric interlayer as a pavement moisture barrier." *Transportation Research Circular E-C006*, Transportation Research Board, Washington, D.C.
- Phillips, P. (1993). "Long term performance of geotextile reinforced seals to control shrinkage on stabilized and unstable clay bases." *Proc., 2nd International RILEM Conference – Reflective Cracking in Pavements*, E & FN Spon, Liege, Belgium, 406-412.
- Scuero, A., and Vaschetti, G. L. (1997). "Polyvinylchloride geocomposites as a barrier to seepage and deterioration of old and new dams." *Geosynthetics Asia*, Bangalore, India.
- Topp, G. C., Davis, J. L., and Annan, A. P. (1980). "Electromagnetic determination of soil water content: measurements in coaxial transmission lines." *Water Resources Research*, Vol.16, 574-582.
- Ullidtz, P. (1987). *Pavement Analysis*, Elsevier Science, New York, NY.
- Wanamakok, P., Martinez, J. C., Al-Qadi, I. L., and Wilkes, J. A. (2001). "Use of discrete event simulation to design geocomposite membrane installations." *Journal of the Transportation Research Record 1772*, Transportation Research Board, Washington, D.C., 197-202.